Submitted to
Journal of Applied Physics

LBL-1843
Preprint c.1

# PRISMATIC DISLOCATION LOOPS ON IMPURITY PRECIPITATES IN MAGNESIUM OXIDE SINGLE CRYSTALS

J. Narayan

January 1973

Prepared for the U.S. Atomic Energy Commission
under Contract W-7405-ENG-48

For Reference

Not to be taken from this room

LAWRENCE BERKELEY LABORATORY
UNIVERSITY OF CALIFORNIA
BERKELEY

LBL-1843
c.1

## DISCLAIMER

This document was prepared as an account of work sponsored by the United States Government. While this document is believed to contain correct information, neither the United States Government nor any agency thereof, nor the Regents of the University of California, nor any of their employees, makes any warranty, express or implied, or assumes any legal responsibility for the accuracy, completeness, or usefulness of any information, apparatus, product, or process disclosed, or represents that its use would not infringe privately owned rights. Reference herein to any specific commercial product, process, or service by its trade name, trademark, manufacturer, or otherwise, does not necessarily constitute or imply its endorsement, recommendation, or favoring by the United States Government or any agency thereof, or the Regents of the University of California. The views and opinions of authors expressed herein do not necessarily state or reflect those of the United States Government or any agency thereof or the Regents of the University of California.

0 0 0 0 3 9 0 0 8 1 3



# PRISMATIC DISLOCATION LOOPS ON IMPURITY PRECIPITATES IN MAGNESIUM OXIDE SINGLE CRYSTALS

J. Narayan*

Inorganic Materials Research Division, Lawrence Berkeley Laboratory and Department of Materials Science and Engineering, College of Engineering; University of California, Berkeley, California 94720

## ABSTRACT

Prismatic dislocation loops, $b = \frac{1}{2}$ <101>, were observed around impurity precipitates in as-grown magnesium oxide single crystals with a high percentage of Ca and Al impurities. The loops lay on {101} slip planes. By using the results of dynamical theory of electron diffraction including absorption, the majority of the loops were identified as $b = \frac{1}{2}$ <101> vacancy type. The possible chemical form of these impurities is discussed in view of the nature of the dislocation loops.

---

*Present address: Solid State Division, Oak Ridge National Laboratory, Oak Ridge, Tennessee 37830.

## INTRODUCTION

Impurity precipitates in single crystals of magnesium oxide have been studied by several investigators.[1-5] Still identification is often lacking because of varying concentrations of impurities in different batches of crystals. There is also some controversy as to whether or not these precipitate particles can act as dislocation sources and consequently affect the yield stress.[4,6] In ionic solids of rock salt structure, the grown-in network of dislocations appears to play no role in plastic deformation. Therefore, the Frank-Read mechanism as the source of dislocations is not important in rock salt structure ionic solids.[6-8] To explain the comparatively low yield stress of lithium fluoride it was proposed by a number of investigators[9-12] that prismatic loops formed by vacancy condensation around precipitates were acting either directly or indirectly as the dislocation sources. However, no direct evidence for the formation of prismatic dislocation loops around precipitates has been previously presented. The present report provides such evidence for MgO. From the nature of the dislocation loops at precipitate particles, one can determine the sign and magnitude of the local stress field and consequently the possible chemical form of the precipitates.

## EXPERIMENTAL

Two grades of large grained polycrystalline MgO were obtained from Muscle Shoals Electro-chemical Corporation, Tuscumbia, Alabama. The results of quantitative analysis done by Coors, Spectro-chemical Laboratory, Golden, Colorado, on samples No. 1 and No. 2 are included in Table I as well as the impurity content reported for specimens studied by Henderson.[3]

Single crystal specimens in the form of thin sheets (0.5 - 1.0 mm thick) were obtained by cleaving along {001} planes. The surface damage introduced during cleaving was removed by chemical polishing in hot orthophosphoric acid (150-160°C) to a thickness of about 0.1 mm. Thin foils for the electron microscope were obtained using the jet polishing technique.[13] All the foils were examined in a Siemens electron microscope at 100 kV.

## RESULTS AND DISCUSSION

Rock salt structure ionic solids have six slip systems of {110} $\langle\bar{1}10\rangle$ type, each slip plane of the type {110} having only one slip vector $\frac{1}{2}\langle\bar{1}10\rangle$. Studies have been made on MgO of two grades (MgO No. 1 and MgO No. 2, see experimental section) having different chemical composition and probably different thermal histories. In MgO No. 1, there were two batches of samples. Figures 1 and 2 shown below are from the first batch and the rest are from the second batch.

The dislocation loop A (Fig. 1a) is in contrast for diffraction vector g = [200]. For the loops $b = \frac{1}{2}[011]$ or $b = \frac{1}{2}[0\bar{1}1]$, $\bar{g}\cdot\bar{b} = 0$ and for the loops $b = \frac{1}{2}[110]$ or $b = \frac{1}{2}[\bar{1}10]$, the loop should appear as a line because the electron beam is parallel to [001]. Therefore the loop in contrast for g = [200] should have as a b-vector either $\frac{1}{2}[101]$ or $\frac{1}{2}[\bar{1}01]$. This is confirmed from Fig. 1b where the same area is shown for g = [020]. The dislocation loop A is out of contrast because $\bar{g}\cdot\bar{b} = 0$,[14] but the dislocation loop B now is in contrast with $b = \frac{1}{2}[011]$ or $\frac{1}{2}[0\bar{1}1]$. The loop B does not project as a line, so it can have neither $\frac{1}{2}[110]$ nor

$\frac{1}{2}$ [$\bar{1}$10] as a b-vector. The residual contrast of the loop A in Fig. 1b is due to $\bar{g}\cdot\bar{b} \times \bar{u}$ component,[14] where $\bar{u}$ is the tangent vector to the dislocation line. In the same foil, the dislocation loop C is in contrast for g = [020] having b = $\frac{1}{2}$ [011] or $\frac{1}{2}$ [01$\bar{1}$]. Figure 2 shows electron micrographs from a similar batch of MgO. The dislocation loops A (Fig. 2a) and C (Fig. 2b) are in contrast for g = [200]. From the same arguments as given for the loops in Fig. 1, these have a b-vector equal to either $\frac{1}{2}$ [101] or $\frac{1}{2}$ [$\bar{1}$01]. The loops at B and D with b = $\frac{1}{2}$[011] or $\frac{1}{2}$[0$\bar{1}$1] are out of contrast because $\bar{g}\cdot\bar{b}$ = 0. The loop E (Fig. 2c) is very near an impurity precipitate but is not attached to it probably because the dislocation loop is of an interstitial type. This point will be discussed below.

Figures 3a and 3b are from the same area of a foil. The dislocation loops A and C (Fig. 3a) are in contrast for g = [200] and the loop B (Fig. 3b) is in contrast for g = [020]. Therefore the loops A and B have b-vector $\frac{1}{2}$ [101] or $\frac{1}{2}$ [$\bar{1}$01] and C has b-vector $\frac{1}{2}$ [011] or $\frac{1}{2}$ [0$\bar{1}$1]. Again the residual contrast for $\bar{g}\cdot\bar{b}$ = 0 is due to the $\bar{g}\cdot\bar{b} \times \bar{u}$ component. The loops D, E and F (Fig. 3c) are in contrast for g = [200]. These appear almost in a line. This is expected for loops on (110) and ($\bar{1}$10) planes when projected on a (001) plane (i.e., electron beam being almost parallel to [001] direction). The loops H and I are in contrast having b = $\frac{1}{2}$ [$\bar{1}$01] or $\frac{1}{2}$ [101] and the loop G, being out of contrast for g = [200], should have b = $\frac{1}{2}$ [011] or $\frac{1}{2}$ [0$\bar{1}$1]. Figure 4 is from a similar batch of samples as Fig. 3. The loops at A (Fig. 4a) having b = $\frac{1}{2}$ [101] or $\frac{1}{2}$ [$\bar{1}$01] grew on the same precipitate but could not combine because they probably lie on different atomic layers and have repulsive interaction.[15] Besides, MgO has higher lattice frictional stress compared to metals.[16]

The loops at B (Fig. 4b) with $\frac{1}{2}$ [011] or $\frac{1}{2}$ [0$\bar{1}$1] probably lie on different parallel atomic layers because both the loops have similar (inside the extra half plane) contrast.[14] In Fig. 4c, the loops A, B, and C have either b = $\frac{1}{2}$ [101], $\frac{1}{2}$ [$\bar{1}$01] and the loop at E, which is out of contrast has b = $\frac{1}{2}$ [011] or $\frac{1}{2}$ [0$\bar{1}$1].

Sometimes loops grow on all six {110} planes around impurities, see A in Fig. 5a . Figure 5a is for the diffraction vector [200] imaging loops of b-vectors $\frac{1}{2}$ [101], $\frac{1}{2}$ [$\bar{1}$01] and $\frac{1}{2}$ [110], $\frac{1}{2}$ [$\bar{1}$10] and 5d is for the diffraction [020] imaging loops with b-vectors $\frac{1}{2}$ [011], $\frac{1}{2}$ [0$\bar{1}$1] and $\frac{1}{2}$ [110], $\frac{1}{2}$ [$\bar{1}$10]. Therefore, the common portion between Figs. 5a and 5d has a b-vector equal to $\frac{1}{2}$ [110] or $\frac{1}{2}$ [110], and the part appearing exclusively in Fig. 5a has a b-vector equal to $\frac{1}{2}$ [101] or $\frac{1}{2}$ [$\bar{1}$01]. That appearing exclusively in Fig. 5d has a b-vector equal to $\frac{1}{2}$ [011] or $\frac{1}{2}$ [0$\bar{1}$1]. Figures 5a and 5c are stereo pairs giving three-dimensional views which confirm the above analysis. Notice that the loop C and the dipole with b = $\frac{1}{2}$ [101] or $\frac{1}{2}$ [$\bar{1}$01] (Fig. 5a) are out of contrast for g = [020] in Fig. 5d.

A method[17] based on dynamical theory of electron diffraction with absorption was used to determine the plane and subsequently the nature of the loop (interstitial or vacancy). When the diffraction vector is changed from g = [200] to g = [$\bar{2}$00], the size of the loop decreases (Fig. 6a and 6b). From Fig. 6c, the slope of the plane on which the loop lies is known because for a dark field picture the top of the foil is in better contrast when S (the deviation from the Bragg angle) is negative. For dark field S positive, the bottom of the foil is in better contrast (Fig. 6d), and for S more positive (Fig. 6e), the top is out of contrast. Therefore out of the four

possibilities shown in Fig. 7, the loop in Fig. 6 corresponds to case III. Eight dislocation loops associated with impurities were analysed by this method and all were found to be vacancy type.

From the nature of dislocation loops, the possible chemical form of the impurities can be predicted. MgO as-supplied was large-grained polycrystalline and was manufactured by controlled cooling of a large mass of MgO. During cooling, precipitates with a lower coefficient of expansion than the matrix have compressive stresses and therefore can act as favorable sites for excess vacancies. Previous electron diffraction experiments have identified precipitates in MgO, $MgO \cdot Al_2O_3$ spinel (Henderson[3]), and $ZrO_2$ particles with some calcium (Venables[2]).

In the present experiments, the precipitate particles are most likely $MgO \cdot Al_2O_3$ spinel for the following reasons:

(i) Since the coefficient of thermal expansion of $MgO \cdot Al_2O_3$ is $9 \times 10^{-6}$, which is less than that of MgO ($14 \times 10^{-6}$), compressive stresses are introduced during cooling. Therefore, vacancies should be attracted toward $MgO \cdot Al_2O_3$ particles. On the other hand, the coefficient of thermal expansion of $ZrO_2$ is $30 \times 10^{-6}$, which leads to hydrostatic tension on cooling. In this case, vacancies should be repelled.

(ii) No loops associated with the impurity particles were found in MgO sample No. 2 which contained less Ca and Al. This suggests that either Ca or Al was important for the formation of loops.

(iii) As shown in section 3, concentrations of the two impurities Ca and Al in MgO sample No. 1 were approximately the same as in the material used by Henderson.[3] He concluded that $MgO \cdot Al_2O_3$ was the most likely precipitate.

Further evidence is shown in Fig. 5. The size of the dislocation loop C, very near the impurity precipitate decreases from diffraction vector [200] (Fig. 5a) to [$\bar{2}$00] (Fig. 5b). From a knowledge of the slope of the plane of the loop(from the stereo pair Figs. 5a and c), loop C was determined to be an interstitial type. The dislocation loop C is very near to the precipitate but is not attached to it. This can be explained if the precipitate is $MgO \cdot Al_2O_3$ so that interstitial loop C experiences a net repulsion. Probably loop E in Fig. 2c is also an interstitial type. These interstitial loops may have been produced by a prismatic punching mechanism due to compressive stresses introduced during cooling of the crystal. Support for this hypothesis is obtained from the observation that the sizes of the interstitial loops are approximately equal to the precipitate sizes respectively in both cases. Thus, prismatic loops generated by a punching mechanism are constrained to be not much different in size than the precipitate that leads to their formation. (A sphere can produce prismatic loops with the diameter equal to its own. A rod can generate prismatic loops with a diameter corresponding to its length and diameter. Finally, a platelet can produce circular loops corresponding to its largest dimension.)

Figure 8 shows an interstitial loop inside a vacancy loop. This was confirmed by determining the change in the size of the loop from diffraction condition g = [200] (Fig. 8a) to g = [$\bar{2}$00] (Fig. 8b) and finding the slope of the plane from the stereo pair (Fig. 8a and Fig. 8c). For g = [020] both of them vanish and a loop, which is in faint

contrast in Fig. 8a, appears in contrast. This configuration probably results when multiple loops are nucleated at a precipitate. If the cooling rate is fast enough, different parts of the loops may grow rapidly and surround an area with very few vacancies, forming an interstitial loop inside a vacancy loop, as shown schematically in Fig. 9.

The precipitates were observed to be inside or at the circumference of the loop. The position of the dislocation loop relative to the precipitate probably depends on the size and shape of the particle, the rate of pipe diffusion[18] of vacancies along the dislocation, and the nearby vacancy supersaturation during growth of the loop. If pipe diffusion is rapid enough compared to the rate of vacancy diffusion into the dislocation loop during growth, it remains circular and in contact with the precipitate. Otherwise at some stage the dislocation line may bow around the impurity and break away from it leaving the precipitate inside the loop (notable examples: loops B and G in Fig. 3).

Occasionally if impurities are near each other, dislocation loops nucleate and grow separately at impurities and may coalesce to form one loop eventually (notable examples: loops A and H in Fig. 3 and A, B and C in Fig. 4c). Two prismatic dislocation loops can have either an attractive or repulsive interaction depending upon the relative location of one loop with respect to the other loop. Apparently the constituent loops of loops A and H in Fig. 3 and A, B and C in Fig. 4c had an attractive interaction and therefore coalesced to form single loops. In contrast to this, the loops at A in Fig. 4a and at B in Fig. 4b could not coalesce to form single loops probably due to a repulsive interaction.

The sizes of the dislocation loops and impurity precipitates seem to be critically dictated by the prior history of the samples. In the growth of MgO, a large mass of MgO mostly in the powder form is melted and cooled slowly to get large-grained polycrystalline material. MgO crystals are obtained by separating and appropriately cleaving along {100} planes. The observed prismatic loops are formed due to vacancy coalescence during the cooling phase of the crystal growth process.
This may be one of the reasons why loop size is different in two batches of the samples with the same impurity content. Also, Henderson,[3] unlike Bowen and Clarke,[4] reported incoherent impurity precipitates with dislocation around the crystals of similar impurity content.

## CONCLUSIONS

(i) Prismatic edge dislocation loops which grow around impurity precipitates lie on {110} slip planes and the majority of the loops are vacancy type.

(ii) Impurities associated with the prismatic dislocation loops appear to be $MgO \cdot Al_2O_3$.

(iii) The position of the impurity particle in relation to the loop depends upon the local supersaturation of vacancies and the ease of the pipe diffusion.

## ACKNOWLEDGMENTS

The author wishes to thank Prof. J. Washburn and Drs. S. M. Ohr and H. D. Guberman for helpful comments on the manuscript.

This work was done under the auspices of the U. S. Atomic Energy Commission.

TABLE I

| Impurities | Amount in ppm MgO No. 1 | Amount in ppm MgO No. 2 | Detection limit of Coors in ppm | Amount in Henderson's MgO |
|---|---|---|---|---|
| Al | 175 | 100 | 1 | 200 |
| Ca | 150 | 50 | 10 | 150 |
| Cu | 20 | 20 | 1 | 2 |
| Fe | 100 | 100 | 1 | 50 |
| Mn | 20 | 20 | 1 | 5 |
| Si | 35 | 75 | 1 | no |
| Mg | major | major | 1 | major |
| Zr | no | no | 10 | no |

Other impurities (ppm) in MgO used by Henderson.[3]

| Zn, Na, Co, Pb | Cd, Ge, Sn, Ga In, Bi, Mo, Ni | Pd, Tl | Ca, Sb, Ti |
|---|---|---|---|
| 20 50 <5 2 | <1 | <2 | <10 |

## REFERENCES


1. J. D. Venables, Phys. Rev. 122, 1388 (1961).
2. J. D. Venables, J. Appl. Phys. 39, 293 (1963).
3. B. Henderson, Phil. Mag. 9, 153 (1964).
4. D. H. Bowen and F. J. P. Clarke, Phil. Mag. 8, 1257 (1963).
5. G. D. Miles, J. Appl. Phys. 36, 1471 (1965).
6. R. J. Stokes, Trans. AIME 224, 1227 (1962).
7. J. J. Gilman and W. G. Johnston: Dislocations and Mechanical Properties of Crystals, John Wiley, p. 116, 1957.
8. J. J. Gilman, J. Appl. Phys. 30, 1584 (1959).
9. J. C. Fisher, Dislocation and Mechanical Properties of Crystals, p. 513, John Wiley, 1957.
10. J. Weertman, J. Appl. Phys. 28, 1068 (1959).
11. J. Gilman, J. Appl. Phys. 30, 1584 (1959).
12. D. Kuhlmann-Wilsdorf, Phil. Mag. 3, 125 (1958).
13. J. Washburn, G. W. Groves, A. Kelly and G. K. Williamson, Phil. Mag. 5, 991 (1960).
14. P. B. Hirsch et al., Electron Microscopy of Thin Crystals, p. 262, Butterworths, 1965.
15. A. J. E. Foreman and J. D. Eshelby, AERE-4170 (1962).
16. J. Narayan, Ph.D. Thesis, (LBL-406), University of California, Berkeley (1971).
17. G. Thomas and W. L. Bell, Proc. Honolulu Conference on Lattice Defects, p. 477, Gordon and Breach, New York, 1967.
18. J. Narayan and J. Washburn, Crystal Lattice Defects 3, 91 (1972).

## FIGURE CAPTIONS

Fig. 1 a) g = [200], the loop A with b = $\frac{1}{2}$ [101] or $\frac{1}{2}$ [$\bar{1}$01] is in contrast. b) g = [020], the same area as a), the loop B with b = $\frac{1}{2}$ [011] or $\frac{1}{2}$ [0$\bar{1}$1] is in contrast. c) loop C with b = $\frac{1}{2}$ [011] or $\frac{1}{2}$ [0$\bar{1}$1] is in contrast.

Fig. 2 g = [200], all the loops have b = $\frac{1}{2}$ [101] or $\frac{1}{2}$ [$\bar{1}$01].

Fig. 3 a) Dislocation loops A and C with $\frac{1}{2}$ [101] or $\frac{1}{2}$ [$\bar{1}$01] are in contrast and the loop B, b = $\frac{1}{2}$ [011] or $\frac{1}{2}$ [0$\bar{1}$1] is out of contrast for g = [200]. b) The same area as a) for g = [020], now loop B is in contrast. c) g = [200], loops D, E and F have b = $\frac{1}{2}$ [110] or $\frac{1}{2}$ [$\bar{1}$10], G has $\frac{1}{2}$ [011] or $\frac{1}{2}$ [0$\bar{1}$1] and loops H and I have b = $\frac{1}{2}$ [101] or $\frac{1}{2}$ [$\bar{1}$01].

Fig. 4 a) g = [200]; two loops at A with b = $\frac{1}{2}$ [101] or $\frac{1}{2}$ [$\bar{1}$01] on different atomic layers. b) g = [020]; two loops at B with b = $\frac{1}{2}$ [011] or $\frac{1}{2}$ [0$\bar{1}$1] on different atomic layers. c) g = [200]; the loops A, B, and C with b = $\frac{1}{2}$ [101] or $\frac{1}{2}$ [$\bar{1}$01], the loop at E with b = $\frac{1}{2}$ [011] or $\frac{1}{2}$ [0$\bar{1}$1].

Fig. 5 a) g = [200], the loops with b = $\frac{1}{2}$ [101] or $\frac{1}{2}$ [$\bar{1}$01] are in contrast. b) g = [$\bar{2}$00]; for the loops b = $\frac{1}{2}$ [101] or $\frac{1}{2}$ [$\bar{1}$01], contrast changes from inside the extra half plane to outside the extra half plane.[13] c) Stereo pair at 15° along 200 Kikichi. d) g band = [020]; notice the disappearance of the dipole and the loop C with b = $\frac{1}{2}$ [101] or $\frac{1}{2}$ [$\bar{1}$01].

0 0 0 0 3 9 0 6 8 1 9



Fig. 6 a) $g = [200]$; the loop with $b = \frac{1}{2}[101]$ or $\frac{1}{2}[\bar{1}01]$ in contrast; b) $g = [\bar{2}00]$; c) dark field $S < 0$; d) S slightly positive; e) $S > 0$.

Fig. 7 I - interstitial loop, II - vacancy loop, III - vacancy loop when the plane is sloping in the opposite direction, IV - interstitial loop.

Fig. 8 a) $g = [\bar{2}00]$; b) $g = [200]$; c) stereo pair at 16° along 200 Kikuchi band; d) $g = [020]$, see the loops with $b = \frac{1}{2}[101]$ or $\frac{1}{2}[\bar{1}01]$ which are in contrast in a), b) and c) disappear.

Fig. 9 Mechanism of formation of an interstitial loop inside a vacancy loop as vacancies diffuse toward the precipitate (see from right to left in the figure).

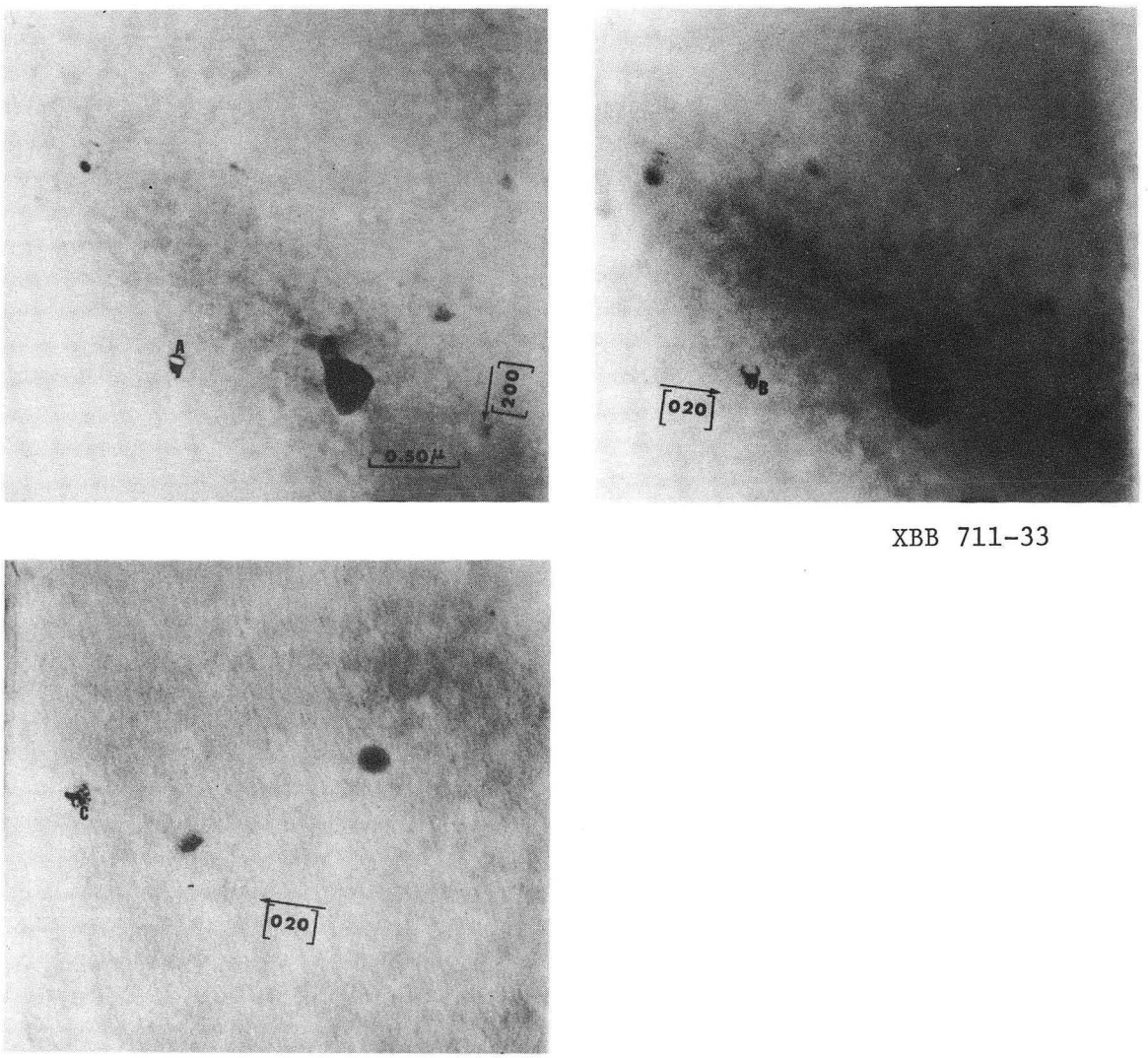


XBB 711-33

Fig. 1.

0 0 0 0 3 9 0 5 8 2 0



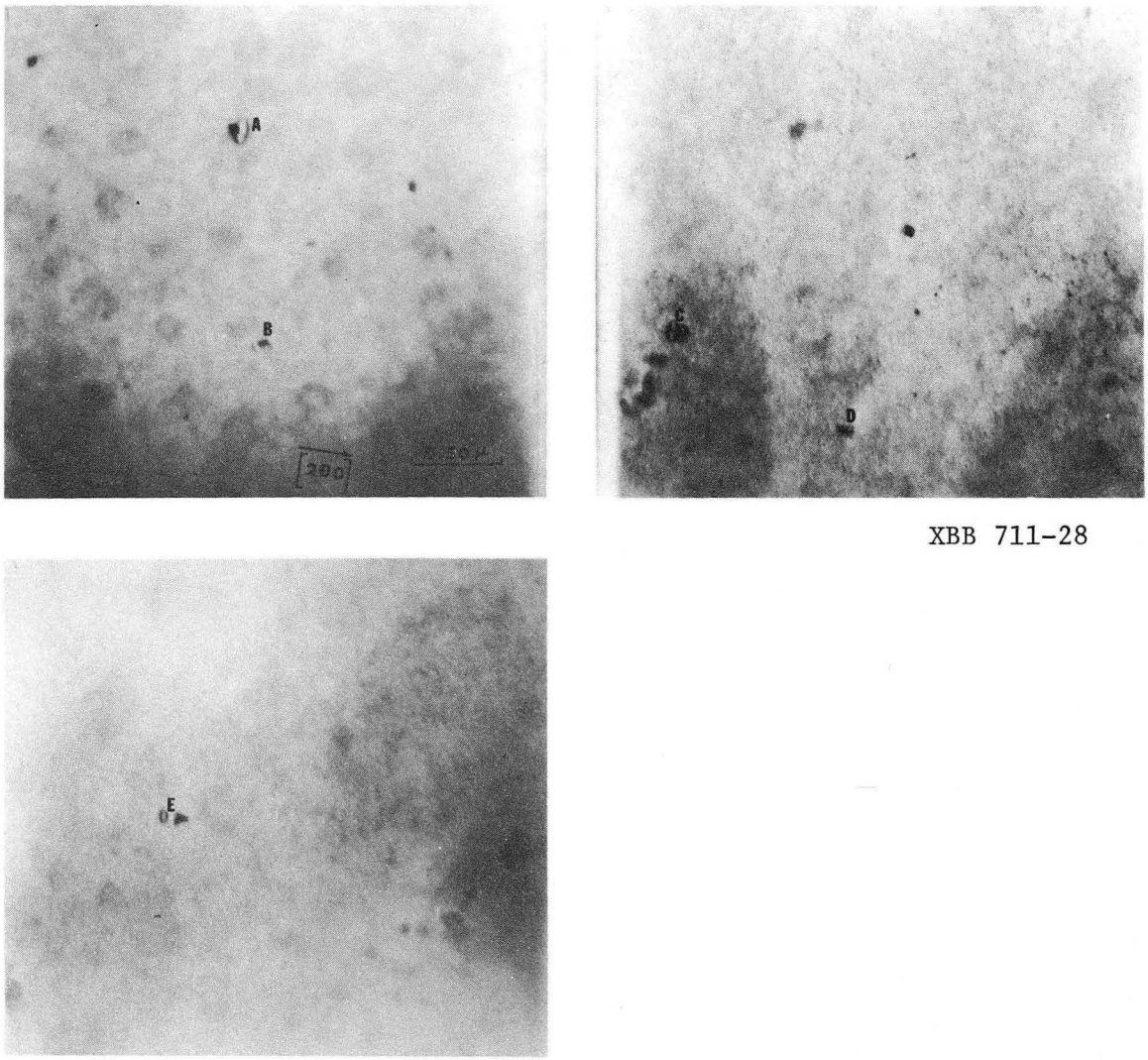


XBB 711-28

Fig. 2.

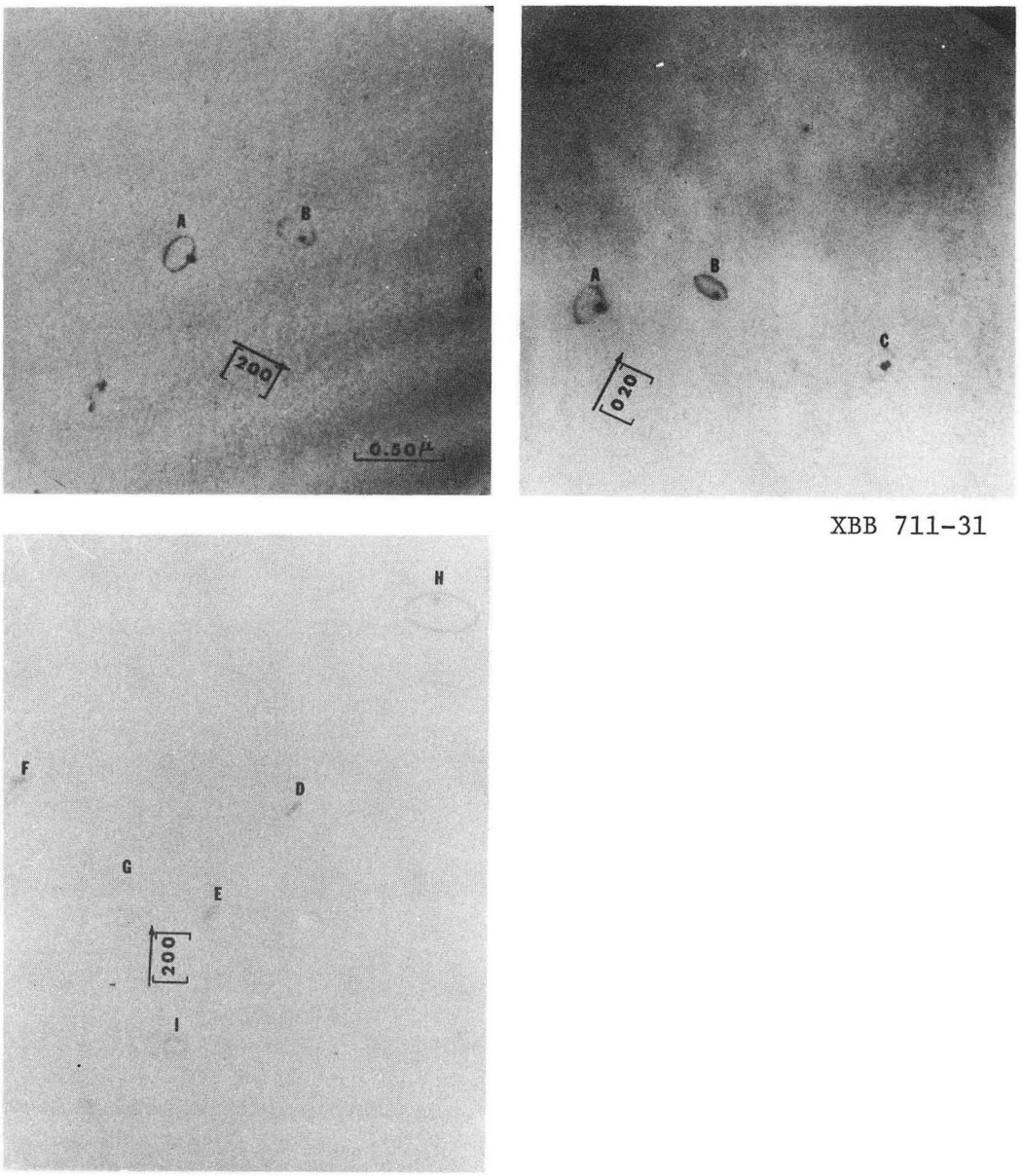


XBB 711-31

Fig. 3.

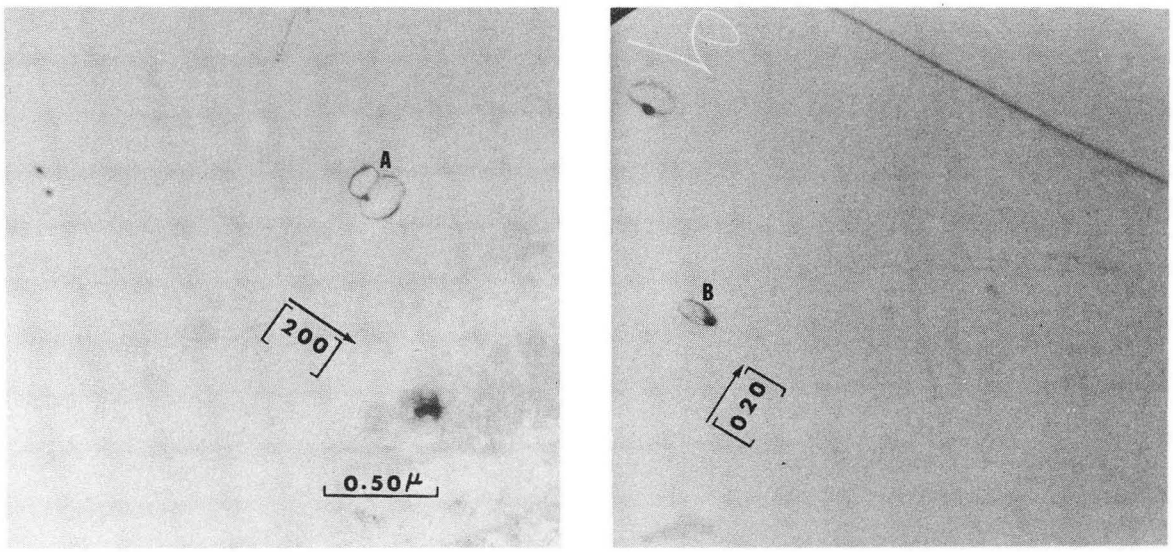


XBB 711-29

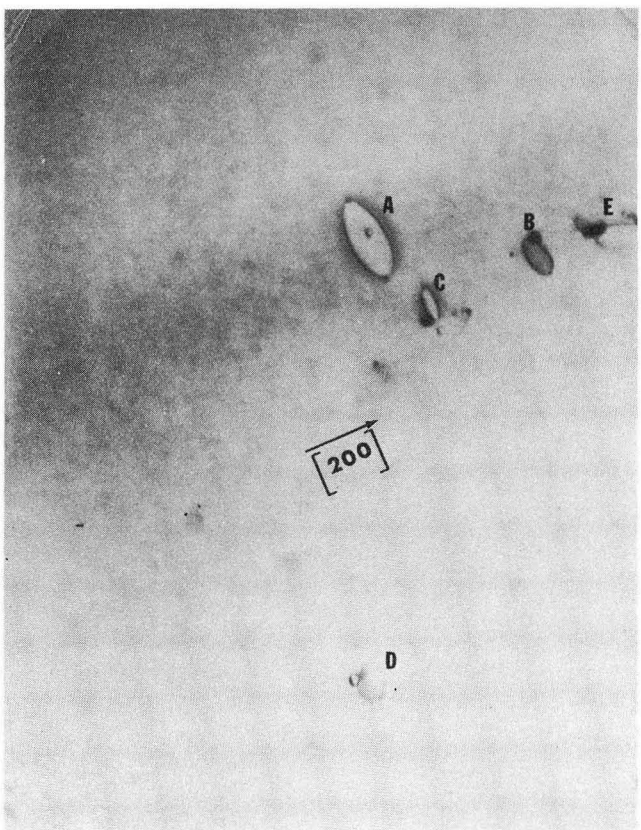


Fig. 4.

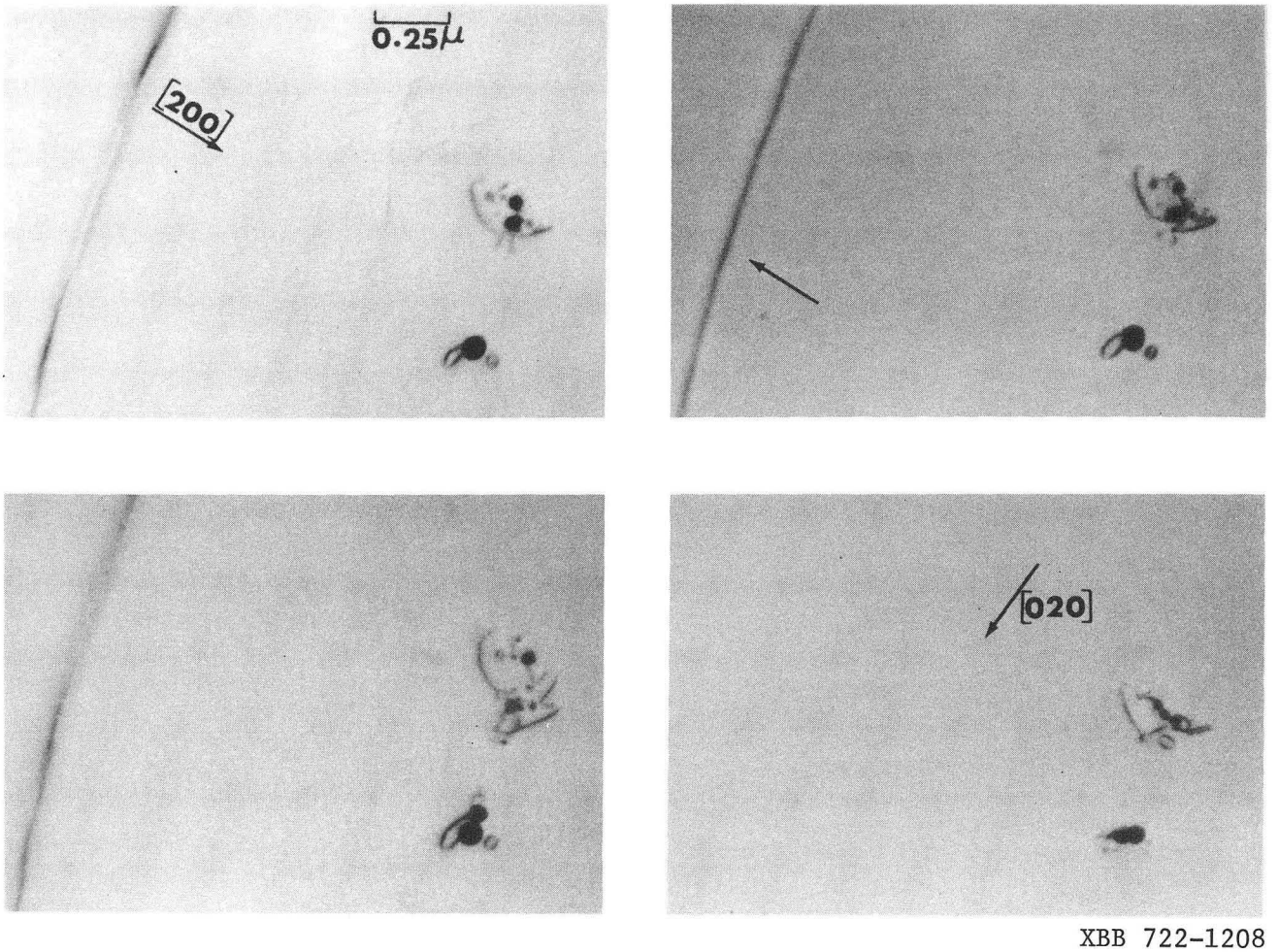


XBB 722-1208

Fig. 5.

0 0 0 0 3 9 0 0 8 2 1



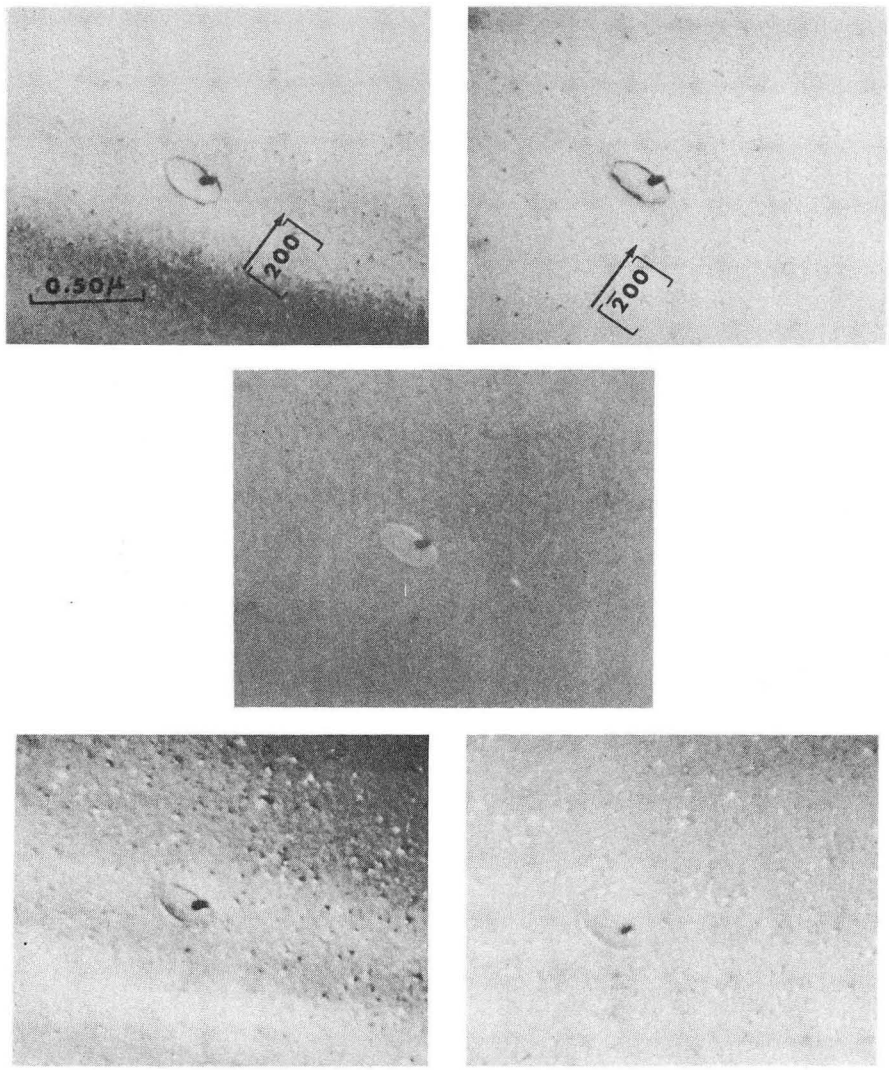


XBB 711-32

Fig. 6.

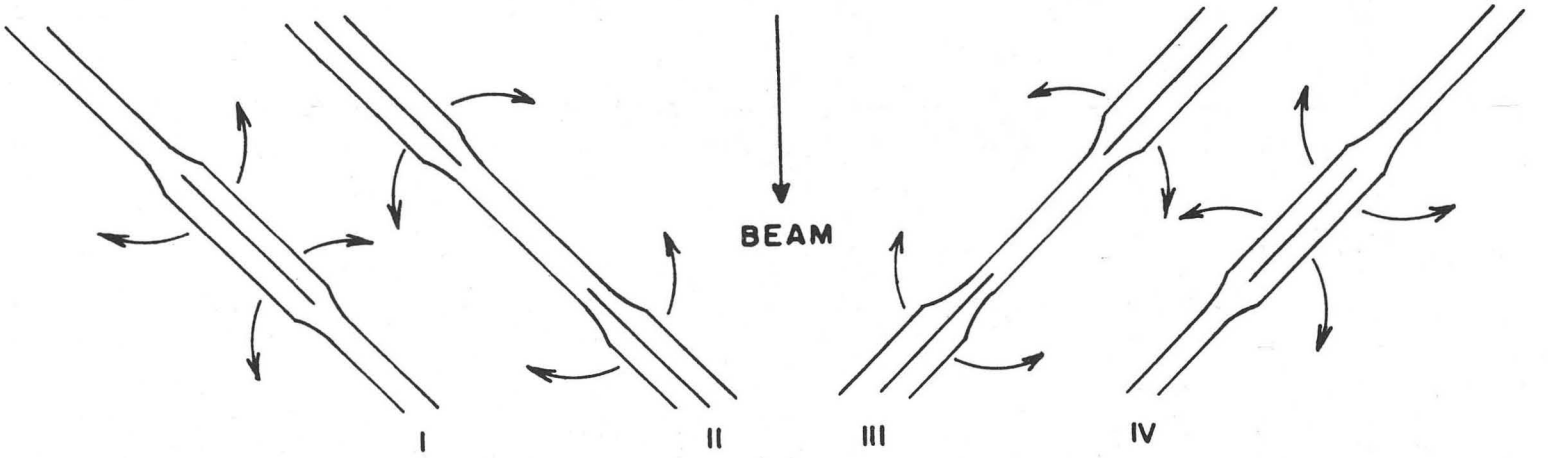


XBL 711-38

Fig. 7.

0 0 0 0 3 9 0 0 8 2 2



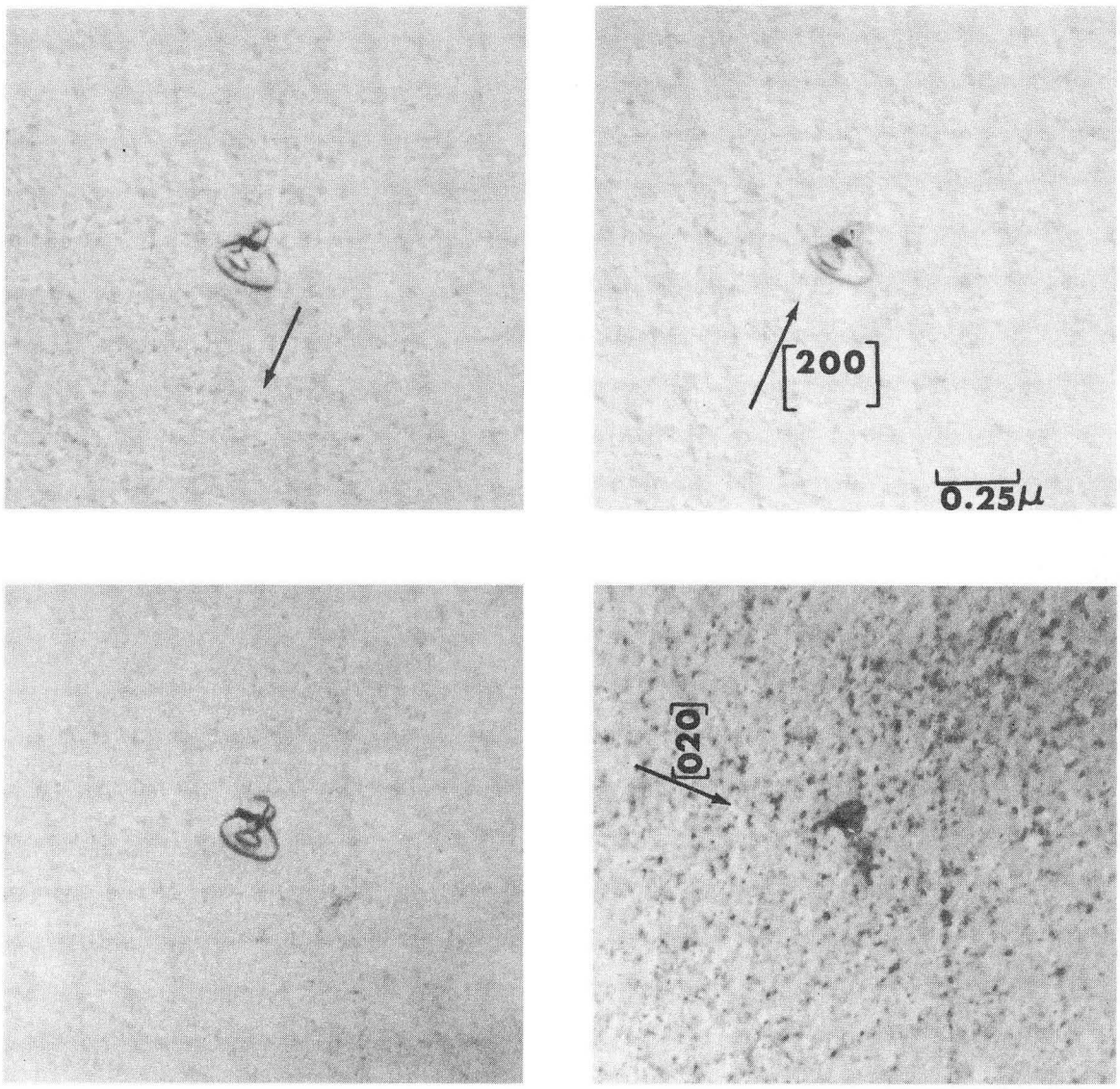


XBB 726-3497

Fig. 8.

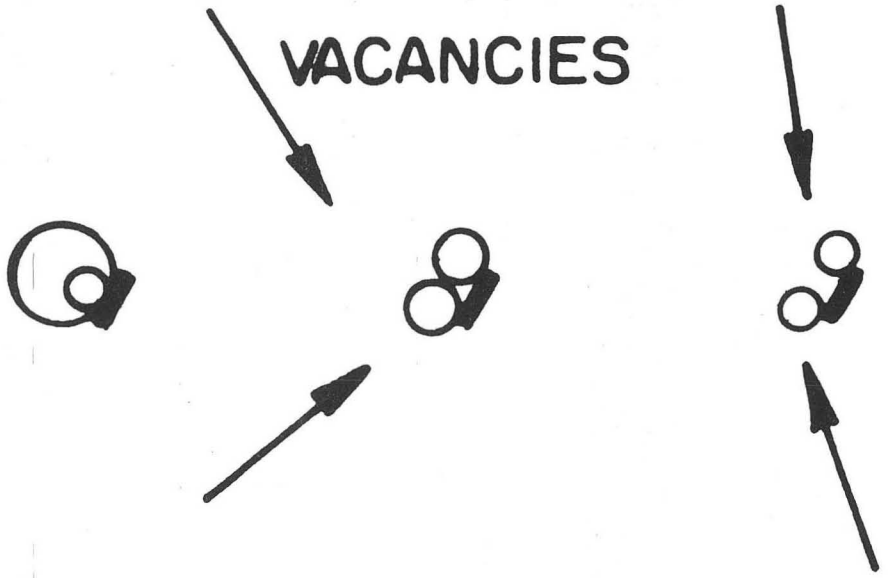


XBL 726-6461

Fig. 9.

LEGAL NOTICE

*This report was prepared as an account of work sponsored by the United States Government. Neither the United States nor the United States Atomic Energy Commission, nor any of their employees, nor any of their contractors, subcontractors, or their employees, makes any warranty, express or implied, or assumes any legal liability or responsibility for the accuracy, completeness or usefulness of any information, apparatus, product or process disclosed, or represents that its use would not infringe privately owned rights.*

*TECHNICAL INFORMATION DIVISION*
*LAWRENCE BERKELEY LABORATORY*
*UNIVERSITY OF CALIFORNIA*
*BERKELEY, CALIFORNIA 94720*